Journal of the European Ceramic Society **14** (1994) 23–27

Low-Shrinkage Refractories by an Infiltration Technique

Nicolas Lequeux, Philippe Larose, Philippe Boch

Laboratoire Céramiques et Matériaux Minéraux, URA-CNRS Matériaux Inorganiques, ESPCI, 10 rue Vauquelin, 75005 Paris, France

&

Nadine Burkarth

Département Matériaux et Procédés, SNECMA, 92234 Gennevilliers, France

(Received 19 November 1993; accepted 1 February 1994)

Abstract

Infiltration of pre-sintered silica + zircon preforms with silica or alumina precursors and subsequent heating lead to the development of crystallized segregations (silica, alumina or mullite), which decreases the sintering shrinkage. The decrease in shrinkage is very sensitive to the nature of segregations.

Die Infiltration von vorgesinterten Silikat + Zirkonsilikat-Ausgangsformen mit Silikat oder Aluminiumoxidvorläufern und anschließendes Erwärmen führte zur Bildung von kristallisierten Ausscheidungen (Silikat, Aluminiumoxid oder Mullit), die das Schrumpfen während des Sinterns vermindern. Die Schrumpfverminderung hängt entscheidend von der Art der Ausscheidung ab.

L'infiltration, par des précurseurs d'alumine ou de silice, de préformes silice + zircon préfrittées, suivie d'un traitement thermique, conduit au développement de ségrégations cristallisées (silice, alumine ou mullite), ce qui décroît le retrait de frittage. Ce retrait s'avère très sensible à la nature des ségrégations.

1 Introduction

Ceramic sintering generally implies shrinkage, which means it is difficult to achieve high accuracy in the shape and size of sintered parts. Machining operations on sintered parts are expensive and difficult to use when the parts have a complicated shape. When porous materials can be accepted, a zero-shrinkage process is the best way for producing net-shaped ceramics. An example is given by the refractory cores which are used for casting the superalloy blades for turbine engines. The cores are made of mixtures of vitreous silica with refractory grains. After sintering, the grains are bonded by necks formed through the viscous flow of vitreous silica. High-temperature treatments lead to the devitrification of silica, which allows the formation of a low-diffusion, low-shrinkage skeleton of cristobalite.[1] The whole shrinkage is below 3%.

The present study was devoted to the preparation of silica + zircon refractories using an infiltration technique inspired by that described in Ref 2–5, with the objective of a decrease in shrinkage.

2 Experimental

2.1 Skeleton preparation

Two industrial compositions (SNECMA, France) were studied. Composition (i) was mostly made of vitreous silica (mean diameter = 19 μm) and zircon (mean diameter = 12 μm) powders. Composition (ii) was similar to (i) except that a small proportion of vitreous silica was replaced by cristobalite (mean diameter = 3 μm). The powders were mixed with a poly(ethylene glycol) binder, then injection molded to form cylinders (0·7 cm × 10 cm). The binder was pyrolyzed by slowly heating the materials from room temperature to 500°C. Then, a presintering treatment was carried out at 1100°C for 5 h. At this stage, the linear shrinkage was below 0·4% and the porosity, measured by the Archimedes technique, was of about 34%.

Journal of the European Ceramic Society 0955-2219/94/$7.00

Table 1. Infiltrates

Starting materials	*Composition (wt%)*		*(Al_2O_3 + SiO_2) equivalent in the precursor (wt %)*	*Mass of solid introduced into the preform by infiltration (wt %)*[a]
	Al_2O_3	*SiO_2*		
Silica sol[b]		100	40	8·7–9·5
Boehmite sol[c]	100		10	3
Silica sol[b] + boehmite sol[c]	71·8	28·2	13·9	3–3·5
Silica sol[b] + aluminum nitrate[d]	71·8	28·2	11·1	2·6

[a] 24 h infiltration; decomposition of precursors at $T > 1100$°C.
[b] Ludox AS40 (Dupont de Nemours).
[c] Dispersal Sol-P3 (Condea Chimie).
[d] Merck 1063.

2.2 Infiltrate preparation

Four infiltrates were prepared using various precursors, as indicated in Table 1. The silica infiltrate was a colloidal sol (Ludox AS40). The alumina infiltrate was made by dispersing 15·4% of a boehmite (AlOOH) powder into a water:acetic acid mixture (H_2O:CH_3COOH = 1:0·002, in molar ratio). The two mullitic infiltrates were made by mixing alumina and silica precursors in the mullite ratio (3 Al_2O_3:2 SiO_2). The first mullitic infiltrate was made by slowly pouring the boehmite sol into the silica sol, keeping the pH at a value between 3 and 4 by adding concentrated hydrochloric acid to avoid gelation. The stability of this mixed sol was low and its gelation occurred in less than 48 h. However, the increase in viscosity associated with gelation was slow enough to allow the infiltration process to be conducted. The second mullitic precursor was made by mixing aluminum nitrate with the silica sol. After a complete dissolution of 100 g of aluminum nitrate into 58 g of water, 13·3 g of silica sol were added to the solution with vigorous stirring. The suspension did not exhibit any gelation effect, even after a time of several months.

2.3 Infiltration procedure

The presintered, porous preforms were immersed into the infiltrates for times ranging from 1 to 3 days, then dried at 110°C. The amount of infiltrate left inside a preform after infiltration was determined using weight measurement. It was found that the volumic fraction of pores that had been impregnated was always greater than 90%. In-situ Archimedes displacement for samples made of material (i) immersed into the silica sol showed that 80% of the porosity was filled in 4 min but that a complete infiltration required a much longer time (several hours). This was related to the necessity of eliminating the air that had been trapped within the smallest pores. The weight gain associated with infiltration (Table 1) was measured after thermal treatments conducted at temperatures ranging from 1100°C to 1500°C, which were high enough to allow full decomposition of precursors and complete elimination of their volatile fraction. The weight data also showed that when the infiltrate was the mixture of silica and aluminum nitrate, the drying treatment resulted in a loss of solid. This loss was due to a migration of the infiltrate toward the surface of the preform during the drying stage, with subsequent removal of the superficial layer of crystallized aluminum nitrate.

2.4 Materials characterization

Linear shrinkage was measured using an absolute dilatometer (Unitherm 1161, Anter Labs, USA), during heating from room temperature to 1500°C, at a rate of 3°C min^{-1}. Room-temperature quantitative X-ray diffraction (CuK_α radiation, Philips PW 1710, Holland) was used to study the devitrification of vitreous silica into cristobalite in materials heated at 3°C min^{-1} to 1200°C, 1275°C, or 1350°C, then cooled rapidly. The ratio between the area of the (101) peak of α-cristobalite and that of the (200) peak of zircon was compared to the similar ratio of reference samples where the two phases had been mixed in known proportions. The crystallization phenomena in alumina- and mullite-based sols were studied for thermal treatments at 1150°C (18, 60 or 300 min) and 1500°C (6 min). The heating rate was of 20°C min^{-1} from room temperature to the soaking temperature.

3 Results and discussion

Figures 1(A) and 1(B) plot the shrinkage versus temperature ($\Delta l/l_0$ versus T) for materials based on compositions (i) and (ii), respectively. They show that the infiltration treatment allows a noticeable decrease in shrinkage. The materials begin to shrink at about 1250°C, with the exception of the materials infiltrated with the silica sol, which begin to shrink at 1050°C and stop shrinking at 1300°C, and which exhibit higher shrinkage than other infiltrated materials. The lowest shrinkage

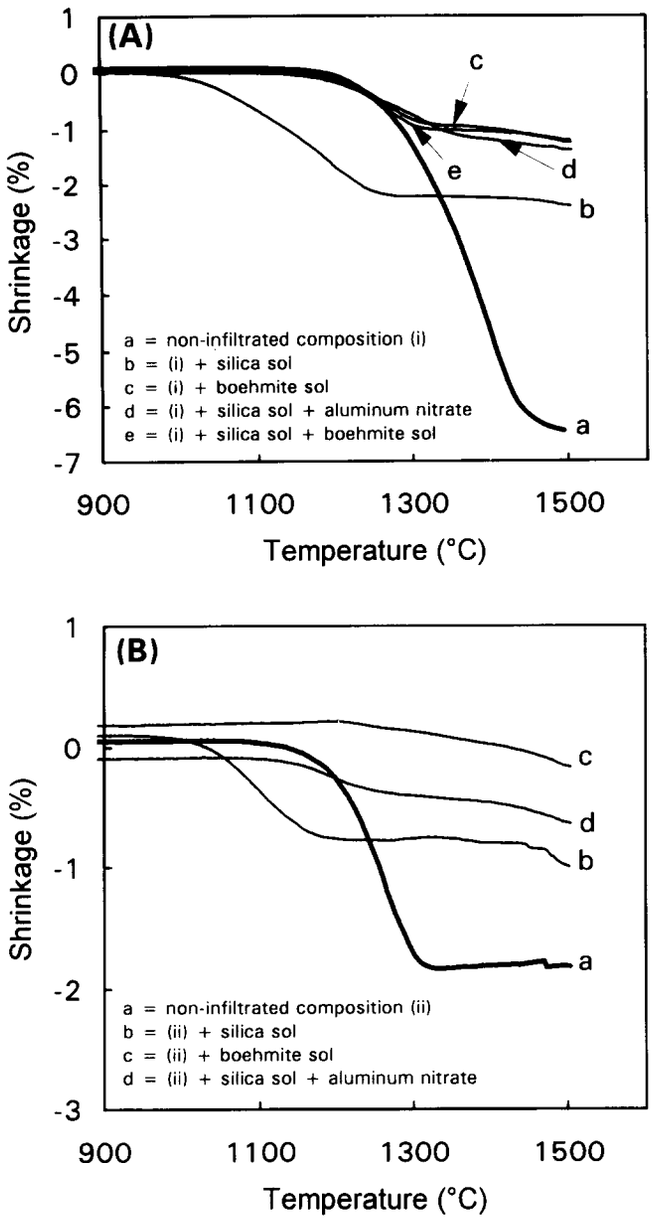

Fig. 1. Shrinkage versus temperature for (A) composition (i) and (B) composition (ii) infiltrated with various precursors.

was obtained when using the boehmite infiltrate. In all cases, material (i) shrinks more than material (ii), which is due to the fact that the latter contains a certain amount of cristobalite in the starting mixture. Figures 2(A)–(D) plot the development of cristobalite versus temperature and the shrinkage rate ($[\delta l/l_0]/\delta T$) versus temperature for materials heated at a constant rate.

3.1 Non-infiltrated materials (Fig. 2(A) and (B))

The devitrification of vitreous silica into cristobalite begins at ≈1275°C in material (i) and at 1200°C in material (ii). Devitrification is more accentuated in the latter material, where the initial cristobalite grains act as nuclei. The shrinkage rate continuously increases with temperature for material (i), whereas it goes through a maximum and then decreases to zero (at $T \approx$ 1350°C) for material (ii).

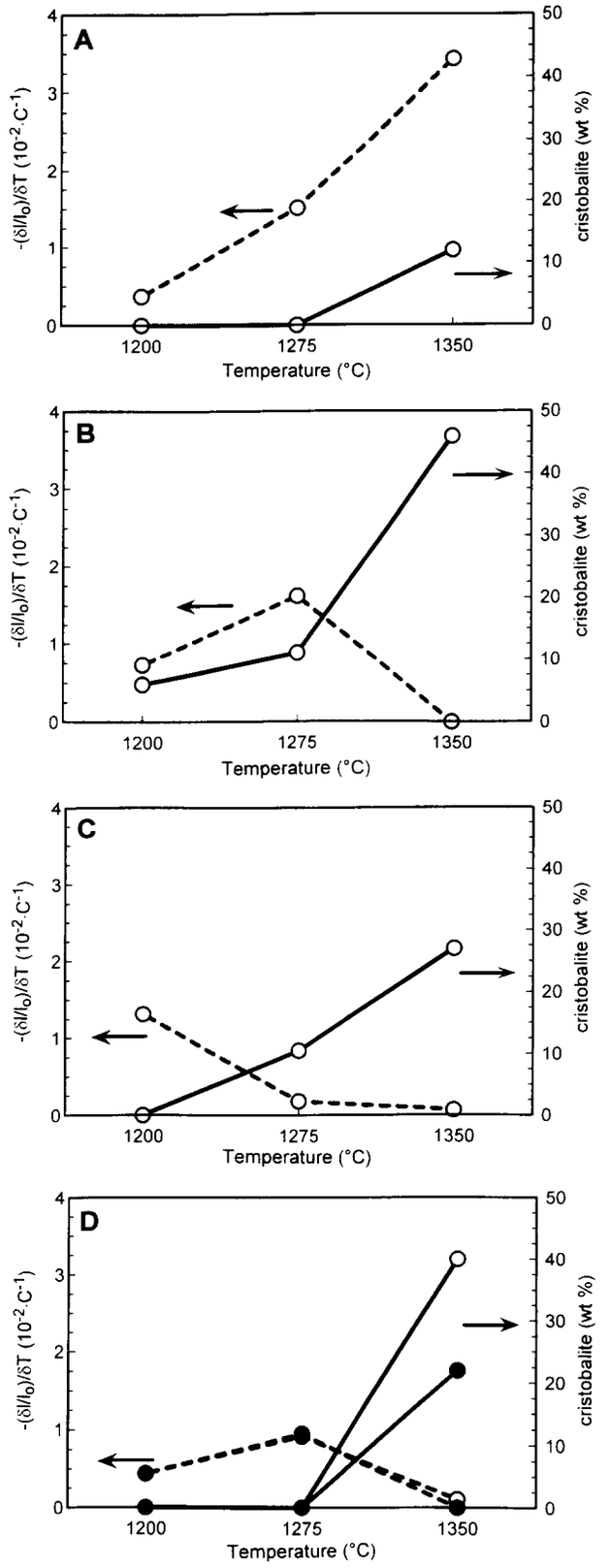

Fig. 2. Shrinkage rate versus temperature and cristobalite/total silica ratio (—) versus temperature, for compositions (i) and (ii) infiltrated with various precursors. (A) composition (i); (B) composition (ii); (C) composition (i) + silica sol; (D) ●, composition (i) + boehmite sol; ○, composition (i) + boehmite sol + silica sol.

3.2 Material (i) infiltrated with the silica sol (Fig 2(C))

Cristobalite begins to form at 1200°C. At 1275°C, the mass of cristobalite is equal to the mass of silica incorporated by infiltration. Comparison with the non-infiltrated material, where devitrification

begins at 1275°C, suggests that it is the colloidal silica that begins to crystallize in infiltrated materials. The shrinkage rate decreases when temperature increases and remains close to zero at $T > 1275$°C.

3.3 Material (i) infiltrated with boehmite or boehmite + silica precursors (Fig. 2(D))

For both infiltrates, the crystallization of cristobalite begins at $T \approx 1275$°C. The shrinkage rate always keeps a low value ($|[\delta l/l_0]/\delta T| < 10^{-2}$ C^{-1}).

Table 2 shows the crystalline phases that are formed from alumina and mullite precursors heated to 1150 and 1500°C for various soaking times. For the boehmite sol, θ-alumina develops first, then α-corundum. For the mullitic mixtures, mullite forms at 1500°C but mullitization is preceded by the formation of a spinel alumina phase at temperatures as low as 1150°C. It was indicated in Refs 6–8 that direct mullitization requires homogeneity at an atomic scale, which can be obtained when using a solution but not when using a suspension. Formation of both α-corundum and cristobalite is observed when the infiltrate is the mixture of silica sol with aluminum nitrate. This indicates that there is a phase separation associated with the recrystallization of aluminum nitrate during the drying stage. A correlation can be established between the value of shrinkage and the nature and amount of the crystalline phases which are formed:

(1) The rate of shrinkage decreases when vitreous silica devitrifies. In industrial casting cores made of silica + zircon grains, it was observed that the crystallization of the vitreous silica grains limits viscous flow phenomena and, therefore, decreases shrinkage.[1] In the present study, material (ii), which contains a small amount of cristobalite in the starting mixtures, exhibits lower shrinkage rates than material (i), at temperatures greater than 1275°C. This shows that the presence of cristobalite grains accelerates the devitrification of vitreous silica. Quantitative data on the cristobalite development during heating show that the initial cristobalite and the ex-precursor phases introduced by infiltration have a similar effect on the devitrification of the vitreous silica grains. However, the infiltration technique does not require the presence of cristobalite in the starting mixtures and, therefore, avoids the formation of cracks caused by the $\alpha \leftrightarrow \beta$ cristobalite transformation that occurs during the cooling stage at the end of the presintering treatment. Consequently, infiltrated materials are expected to exhibit better mechanical properties than conventional ones.

(2) The noticeable shrinkage of materials infiltrated with silica, observed at temperatures between 1050 and 1250°C during experiments conducted at a constant heating rate, is probably due to the viscous flow of the non-recrystallized colloidal silica. This shrinkage does not exist when the silica sol is mixed with the alumina precursors, even though silica does not crystallize. It can be thought that the intimate mixture of boehmite with silica or of aluminum nitrate with silica allows alumina to dissolve into viscous silica. Reactions between alumina and vitreous silica stabilize the precrystallization of alumina into a spinel phase[7]. It is also possible that precrystallization phenomena increase the viscosity of the intergranular phase and, therefore, limit the viscous flow.

(3) The cristobalite that is formed from the colloidal silica is more efficient in decreasing shrinkage than the cristobalite that is introduced into the starting composition. This can be seen by comparing the behavior at

Table 2. Crystalline phases formed when heating the infiltrates to temperatures and for times as indicated

Starting materials	*Crystalline phases*			
	1150°C			*1500°C*
	18 min	*60 min*	*300 min*	*6 min*
Boehmite sol	α-Alumina θ-Alumina[a]	α-Alumina	α-Alumina	α-Alumina
Silica sol + boehmite sol[b]	γ-Alumina(spinel)	γ-Alumina	γ-Alumina	Mullite Cristobalite[b]
Silica sol + aluminum nitrate[b]	α-Alumina γ-Alumina	α-Alumina γ-Alumina	α-Alumina γ-Alumina	Mullite α-Alumina Cristobalite

[a] Traces.
[b] Mullite proportion (Al_2O_3 : SiO_2 = 3:2).

1275°C of material (ii)—which contains initial cristobalite—and of material (i)—which was infiltrated with silica. Even though the content of cristobalite is about the same in both materials, there is a large difference between their shrinkage rates. Infiltration allows the distribution of cristobalite to be more homogeneous and, therefore, more efficient in blocking the particle movements that induce shrinkage.

(4) The incorporation of crystalline phases by infiltration decreases shrinkage. At T = 1275°C, for instance, material (i) infiltrated with alumina or mullite precursors exhibits a lower shrinkage rate than non-infiltrated materials. However, the devitrification of silica is still not observed at this temperature. This shows that the crystallized intergranular segregations themselves (cristobalite, alumina, or mullite) act to limit viscous-flow phenomena. An increase in the length of diffusion paths or a physical constraint between different phases can also explain the hindrance of grain growth, as observed in interconnected composites[9–11]

4 Conclusions

Infiltration of presintered zircon + silica refractories with silica or alumina precursors and subsequent heating lead to the development of silica, alumina or mullite segregations. This leads to a dramatic decrease in the sintering shrinkage, which gives hope to improve precision casting.[12] The decrease in shrinkage is very sensitive to the nature of the crystalline phases that develop during sintering. The main results are:

(1) Shrinkage decreases when
  —the devitrification of vitreous silica increases
  —the infiltrates begin to crystallize.

(2) All the infiltrates accelerate the devitrification of vitreous silica. The initial cristobalite and the ex-precursor segregations play a similar role from this point of view.

(3) Infiltration with the colloidal silica sol leads to a transient shrinkage via viscous flow. The shrinkage develops at $T \geq 1050$°C but it stops when the silica devitrifies.

(4) Shrinkage via transient viscous flow is not observed in silica + alumina infiltrated materials. This can be correlated with the formation of a spinel alumina phase, prior to mullitization.

(5) After crystallization, the infiltrated phases act as boundary segregations and limit viscous flow phenomena.

(6) The lowest shrinkage is observed for the cristobalite-containing composition infiltrated with the alumina precursor: the shrinkage from room temperature to 1500°C (at a heating rate of 3°C min^{-1}) does not exceed 0·1%, whereas it is 1·8% for the non-infiltrated material.

Acknowledgments

This study was supported by SNECMA. The authors gratefully acknowledge P. Chabaneix, T. Bardot, C. Langlois, and P. Calero for their help.

References

1. Huseby, I. C., Borom, M. P. & Greskovich, C. D., High temperature characterization of silica-base cores for superalloys. *Ceram. Bull.*, **58** (1979) 448–52.
2. Marple, B. R. & Green, D. J., Incorporation of mullite as a second phase into alumina by an infiltration technique. *J. Am. Ceram. Soc.*, **71** (1988) C471–3.
3. Marple, B. R. & Green, D. J., Mullite/alumina particules composites by infiltration processing. *J. Am. Ceram. Soc.*, **72** (1989) 2043–8.
4. Marple, B. R. & Green, D. J., Mullite/alumina particules composites by infiltration processing: II, infiltration and characterization. *J. Am. Ceram. Soc.*, **73** (1990) 3611–16.
5. Ravi, V. & Kutty, T. R. N., A novel method for the uniform incorporation of grain-boundary layer modifiers in positive temperature coefficient of resistivity barium titanate. *J. Am. Ceram. Soc.*,.**75** (1992) 203–5.
6. Sacks, M. D., Lee, H. W. & Pask, J. A., A review of powder preparation methods and densification procedures for fabricating high density mullite. In *Proceedings of the International Conference on Mullite*, Vol. 6, ed. American Ceramic Society, Westerville, OH, USA, (1990), pp. 167–207.
7. Aksay, A., Dabbs, D. M. & Sarikaya, M., Mullite for structural, electronic and optical applications. *J. Am. Ceram. Soc.*, **74** (1991) 2343–58.
8. Schneider, H., Merwin, L. & Sebald, A., Mullite formation from non-crystalline precursors. *J. Mat. Sci.*, **27** (1992) 805–12.
9. Lange, F. F., & Hirlinger, M. M., Grain growth in two-phase ceramics: Al_2O_3 inclusions in ZrO_2. *J. Am. Ceram. Soc.*, **70** (1987) 827–30.
10. French, J. D., Harmer, M. P., Chan, H. M. & Miller, G. A., Coarsening-resistant dual-phase interpenetrating microstructures. *J Am. Ceram. Soc.*, **73** (1990) 2508–10.
11. Bordia, K. & Sherer, G. W., On constrained sintering-rigid inclusions. *Acta Metall.*, **36** (1988) 2411–16.
12. SNECMA, pending patent.